(6) (12) R.S.

PHASE RELATIONS IN THE Si_3N_4-SiO_2-MgO SYSTEM AND THEIR INTERRELATIONS WITH STRENGTH AND OXIDATION RESISTANCE,

F. F. Lange

Technical Report #9, September 30, 1976

and

DENSE Si_3N_4: INTERRELATION BETWEEN PHASE EQUILIBRIA, MICROSTRUCTURE AND MECHANICAL PROPERTIES,

(9) Technical rept. no. 9 and Final rept.,

(10) F. F. Lange

FINAL REPORT - September 30, 1976

(11) 30 Sep 76

(12) 54 p.

Westinghouse Electric Corporation
Research and Development Center

(15) Contract Number N00014-74-C-0284,
ARPA Order-2697

Sponsored by the Advanced Projects Agency
ARPA Order Number 2697
Program Code Number 01269

Scientific Officer: Dr. A. M. Diness
Office of Naval Research

Principal Investigator: Dr. F. F. Lange
(412) 256-3554

Effective Date of Contract: April 1, 1974

Contract Expiration Date: June 30, 1976

Amount of Contract: $159,892

Form Approved, Budget -- No. 22-R0293

PHASE RELATIONS IN THE Si_3N_4-SiO_2-MgO SYSTEM AND THEIR INTERRELATIONS WITH STRENGTH AND OXIDATION RESISTANCE

F. F. Lange

Technical Report #9, September 30, 1976

Westinghouse Electric Corporation
Research and Development Center

Contract Number N00014-74-C-0284

Sponsored by the Advanced Projects Agency
ARPA Order Number 2697
Program Code Number 01269

Scientific Officer: Dr. A. M. Diness
Office of Naval Research

Principal Investigator: Dr. F. F. Lange
(412) 256-3554

Effective Date of Contract: April 1, 1974

Contract Expiration Date: June 30, 1976

Amount of Contract: $159,892

Form Approved, Budget -- No. 22-R0293

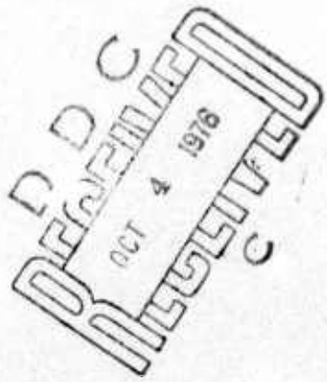

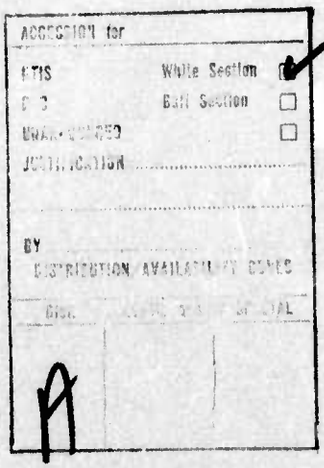

Unclassified

SECURITY CLASSIFICATION OF THIS PAGE *(When Data Entered)*

REPORT DOCUMENTATION PAGE		READ INSTRUCTIONS BEFORE COMPLETING FORM
1. REPORT NUMBER	2. GOVT ACCESSION NO.	3. RECIPIENT'S CATALOG NUMBER
4. TITLE *(and Subtitle)* Phase Relations in the Si_3N_4-SiO_2-MgO System and Their Interrelations with Strength and Oxidation Resistance		5. TYPE OF REPORT & PERIOD COVERED Technical Report #9 September 30, 1976 6. PERFORMING ORG. REPORT NUMBER
7. AUTHOR(s) F. F. Lange		8. CONTRACT OR GRANT NUMBER(s) N00014-74-C-0284
9. PERFORMING ORGANIZATION NAME AND ADDRESS Westinghouse Research Laboratories Beulah Road Pittsburgh, PA 15235		10. PROGRAM ELEMENT, PROJECT, TASK AREA & WORK UNIT NUMBERS
11. CONTROLLING OFFICE NAME AND ADDRESS Dr. A. M. Diness Office of Naval Research Arlington, VA 22217		12. REPORT DATE September 30, 1976 13. NUMBER OF PAGES 19
14. MONITORING AGENCY NAME & ADDRESS*(if different from Controlling Office)*		15. SECURITY CLASS. *(of this report)* Unclassified 15a. DECLASSIFICATION/DOWNGRADING SCHEDULE

16. DISTRIBUTION STATEMENT *(of this Report)*

Reproduction in whole or in part is permitted for any purpose of the U.S. Government. Distribution of this document is UNLIMITED.

17. DISTRIBUTION STATEMENT *(of the abstract entered in Block 20, if different from Report)*

18. SUPPLEMENTARY NOTES

19. KEY WORDS *(Continue on reverse side if necessary and identify by block number)*

Silicon nitride, strength, oxidation, magnesium oxide, silicon dioxide.

20. ABSTRACT *(Continue on reverse side if necessary and identify by block number)*

Phase equilibria studies between 1400°C and 1750°C have established three important tie lines in the Si_3N_4-SiO_2-MgO system, viz., Si_3N_4-MgO, Si_3N_4-Mg_2SiO_4, and Si_2N_2O-Mg_2SiO_4. Strength measurements at 1400°C for fixed Si_3N_4 molar contents and varying MgO/SiO_2 molar ratios show that the maximum high temperature strengths can be obtained for MgO/SiO_2 molar ratios that

DD FORM 1 JAN 73 1473 EDITION OF 1 NOV 65 IS OBSOLETE

Unclassified 376670

SECURITY CLASSIFICATION OF THIS PAGE *(When Data Entered)*

20. (cont'd)

approach zero and infinity. The oxidation of these materials will be discussed in terms of the compatibility of SiO_2 (the oxidation product of Si_3N_4) and the other phases present in the material.

PHASE RELATIONS IN THE Si_3N_4-SiO_2-MgO SYSTEM AND THEIR INTERRELATIONS WITH STRENGTH AND OXIDATION RESISTANCE

F. F. Lange

ABSTRACT

Phase equilibria studies between 1400°C and 1750°C have established three important tie lines in the Si_3N_4-SiO_2-MgO system, viz., Si_3N_4-MgO, Si_3N_4-Mg_2SiO_4, and Si_2N_2O-Mg_2SiO_4. Strength measurements at 1400°C for fixed Si_3N_4 molar contents and varying MgO/SiO_2 molar ratios show that the maximum high temperature strengths can be obtained for MgO/SiO_2 molar ratios that approach zero and infinity. The oxidation of these materials will be discussed in terms of the compatibility of SiO_2 (the oxidation product of Si_3N_4) and the other phases present in the material.

1. INTRODUCTION

Silicon nitride powder consists of both crystalline forms, viz., particles of both α and β structures, and various impurities. Oxygen is by far the largest impurity. The oxygen content of various commercial and non-commercial high α-phase powders range between 0.5 to 3 w/o.[1] Although Jack[2] and co-workers hypothesized that ∿1.5 w/o oxygen was required to stabilize the α-structure, overwhelming evidence[3-7] shows that the α-structure can be a pure Si_3N_4 and that the oxygen is present in the form of either SiO_2, Si_2N_2O, cation-impurity oxides, or complex silicates. Since most powders have insufficient cation-imputiry contents, most of the oxygen must be in the form of either relatively pure SiO_2 or Si_2N_2O. Thus, SiO_2 (or Si_2N_2O) is an important constituent of Si_3N_4 powder, viz., the SiO_2 mole fraction can range between 0.02 to 0.12.

Since Deeley's[8] early work, MgO has been the predominantly used aid to densify Si_3N_4 powder. The MgO is believed to promote a liquid at high temperature which causes densification by a liquid phase sintering phenomenon. It can be hypothesized that all constituents, viz., Si_3N_4, SiO_2, MgO and impurities react at high temperatures to form a liquid and an equilibrium fraction of solid Si_3N_4. After densification and cooling the liquid will solidify to Si_3N_4 and secondary phases. The number, chemistry and content of the secondary phases will depend on the amount of each constituent in the starting powder and the phase relations between the constituents. As experience has shown, the secondary phases can significantly influence all properties.

Although MgO is the most widely used densification aid, the phase relations in the Si_3N_4-SiO_2-MgO system* have never been reported.

*As pointed out by Gauckler[9] et al, one can not apriori consider any Si_3N_4-SiO_2-metal oxide system an ordinary ternary system, e.g., a true binary may not exist along the Si_3N_4-metal oxide join. As it will be shown, the Si_3N_4-SiO_2-MgO system can be represented as an ordinary ternary system.

Oyama and Kamigaito[10] and, more recently, Jack[11] have reported work along the Si_3N_4-MgO join, but in both cases, their work is subject to suspicion since SiO_2 was an unrecognized constituent of the starting powder.

The present work will report the phase relations in the Si_3N_4-SiO_2-MgO system as determined by hot-pressing powders with known constituents and subsequent phase identification by x-ray diffraction analysis. It will be shown that the strength and oxidation resistance of these materials are related to composition. The interrelation between these properties and phase equilibria will be discussed.

2. EXPERIMENTAL

2.1 Starting Powders, Fabrication and Phase Identification

Relatively pure, high α-Si_3N_4 (α/β = 9) powder was used. Cation inpurities are shown in Table 1. The average oxygen content, determined by six analyses* was 0.6 $\pm$ .1 w/o. In preparing compositions it was assumed that the SiO_2 content in the Si_3N_4 was directly related to the oxygen content. Composite powders of Si_3N_4, MgO and SiO_2 were weighed, mixed and milled together as previously described.[11]

The composite powders were densified by hot pressing in grafoil-lined, graphite die with end plungers with 28 MPa in a temperature range of 1500°C to 1750°C† for a period of two hours. After sectioning specimens from each material, a specimen from each composition was annealed in an oxidizing atmosphere at 1000°C for a period of $\geq$ 1000 hours. Phase identification was made by x-ray diffraction analysis of all as-fabricated and many annealed compositions. Polished sections were observed by light microscopy to observe the location of second phases.

2.2 Strength and Oxidation

For the strength and oxidation studies, special compositions were prepared containing 0.91, 0.883 and 0.755 mole fractions of Si_3N_4 and different MgO/SiO_2 molar ratios.

Strength measurements were made at 25°C and 1400°C with a universal testing machine (crosshead speed of 0.005 cm/min) as described previously.[12] Oxidation experiments were carried out in static air at 1375°C. Weight measurements were made after intermittent periods of exposure.

---

*Inert gas diffusion technic (Leico method).

†Powders close to the Si_3N_4-MgO join were fabricated at 1750°C. Most others had to be fabricated at a lower temperature due to an apparently lower liquidus temperature. In several cases, the liquidus was exceeded.

3. RESULTS

3.1 Phase Relations

Figure 1 illustrates the observed tie lines in the Si_3N_4-SiO_2-MgO system along with the compositions used for phase identification. These tie lines appear to be valid over a much wider temperature range than that used for fabrication since no changes were observed after annealing for 1000 hrs at 1000°C. ASTM cards 7-74 and 21-1260 were used to identify Mg_2SiO_4. One or more unidentified phases were observed within the Si_2N_2O-SiO_2-Mg_2SiO_4 phase area. Their identification and relation with other phases were not included in this study.

No solid solution of MgO into the β-Si_3N_4 structure was evident from the x-ray diffraction results.

3.2 Strength Measurements

Figures 2a, b, and c illustrate the flexural strength at 25°C and 1400°C, for the compositions containing 0.91, 0.833 and 0.755 mole fraction Si_3N_4, respectively. All materials indicated in these figures did not absorb water during density measurements and they had a density $\geq$ 3.20 gm/cc.

At 25°C, the strength within each compositional series was not a strong fraction of composition, but the average strength decreased from 780 MPa to 680 MPa from the series containing 0.91 mole fraction Si_3N_4 to the series containing 0.755 Si_3N_4. At 1400°C, a strength minimum was observed in all series for a MgO/SiO_2 molar ratio of ∿2, corrseponding to compositions approaching the Si_3N_4-Mg_2SiO_4 tie line. At this elevated temperature, highest strengths were observed for compositions approaching the Si_3N_4-MgO tie line, and moderately high strengths were observed for MgO/SiO_2 molar ratios between 0.25 and 0.50 corresponding to compositions close to (but not coincident with) the Si_3N_4-Si_2N_2O tie line.

3.3 Oxidation Measurements

Figure 3 illustrates the oxidation kinetics in air at 1375°C for representative compositions from the series of materials containing 0.755 mole fraction Si_3N_4. As illustrated in this weight gain squared vs. time plot, all compositions initially appear to exhibit parabolic rate kinetics. Non-parabolic kinetics is observed after an initial prolonged period for compositions in the 0.755 mole fraction series when the molar content of MgO exceeds ∿0.125. Figure 3 also illustrates that the parabolic rate constant is not a linear fraction of the MgO content. This observation was also made for the series of materials containing 0.91 and 0.833 mole fractions of Si_3N_4.

The total weight gain after 785 hrs in air at 1375°C for the three compositional series is shown in Fig. 4. As shown, materials close to the Si_3N_4-Si_2N_2O tie line exhibited the best resistance to oxidation and materials approaching the Si_3N_4-MgO tie line exhibited the poorest resistance to oxidation. A plateau region in the weight gain vs MgO/SiO_2 ratio appears to exist between the MgO/SiO_2 molar ratios of 0.5 and 2. Materials with a smaller amount of Si_3N_4 exhibited greater oxidation for a given MgO/SiO_2 molar ratio. The surface appearance after prolonged oxidation was indicative of the oxidation resistance of each material, viz., materials close to the Si_3N_4-Si_2N_2O tie line were dark and similar to the unoxidized material; materials close to the Si_3N_4-MgO tie line were light colored, indicative of a thick oxide scale.

Since most materials used to obtain the phase relations shown in Fig. 1 were annealed in air at 1000°C for periods $\geq$ 1000 hrs, the oxidation behavior of materials other than those in the three series shown in Fig. 4 were also observed. The most interesting observation was that the oxide scale almost consumed specimens along the Si_3N_4-MgO tie line for compositions containing $\geq$ 0.60 mole fraction MgO. An x-ray diffraction analysis of these thick oxide scales revealed two forms of Mg_2SiO_4 as the principal oxidation products, viz., forsterite and a cubic, garnet structure ($a_o \simeq 8.11$ Å). The appearance of the garnet structure of Mg_2-SiO_4 was unexpected since it is usually synthesized under high pressure.

4. DISCUSSION

From the data presented above, it is obvious that the high temperature strength and oxidation resistance of hot-pressed Si_3N_4 is strongly dependent on composition. It is also evident that the SiO_2 content of Si_3N_4 powder must be controlled to obtain improved materials and reproducible properties within this system. The following sections will discuss the observed phase relations and strength and oxidation results in terms of phase equilibria. Property optimization will be discussed in a concluding section.

4.1 Phase Relations

Oyama and Kamigaito[10] have studied the Si_3N_4-MgO join with the apparent assumption that SiO_2 was not a constituent in the Si_3N_4 powder. They report that "when MgO concentration was increased, . . . $MgSiN_2$ was found. Further increase of MgO concentration gave rise to the formation of $MgSiN_2$ and $2MgO{\cdot}SiO_2$." They found no changes in the lattice constants of β-Si_3N_4, but they inferred a 0.30 mole fraction solid solution of MgO into Si_3N_4 from thermal expansion measurements.

In the present work, $MgSiN_2$ was never observed; instead, MgO was the major phase (other than β-Si_3N_4) for compositions fabricated along the Si_3N_4-MgO join. Similar to the results of Oyama and Kamigaito[10] no change in the diffraction angles for β-Si_3N_4 were observed in the present work. Since other phases were observed which will influence thermal expansion, the present worker does not believe a change in thermal expansion without a change in lattice constants is indicative of solid solution. In addition, Gauckler[13] et al, have shown that the solid solution of MgO in β-Si_3N_4 is unlikely, unless smaller cations (e.g., Be) are concurrently introduced.

4.2 Strength

It can be postulated that strength degradation within a polyphase material will occur once the solidus temperature is exceeded. Above the solidus temperature a liquid phase will be present due to a reaction of the different phases and the degradation of all mechanical properties would be expected. The amount of liquid present would depend on the temperature in excess of the solidus and the liquidus temperature. Although solidus and eutectic temperature were not systematically determined in this study, observations made during densification indicated that the eutectic temperature along (or close to) the Si_3N_4-Mg_2SiO_4 tie may be as low as 1200°C, viz., rapid densification could be achieved at temperatures as low as 1200°C for compositions on the Mg_2SiO_4 side of the Si_3N_4-Mg_2SiO_4 tie line (see Fig. 1 for compositions) and the liquidus temperature of these same compositions were ∿1500°C. These observations suggest that upon reheating, materials on (or close to) the Si_3N_4-Mg_2SiO_4 tie line, a liquid will develop within the hot-pressed material at relatively low temperatures. This argument points to the need for determining solidus temperatures in this and other Si_3N_4 systems.

Another explanation of the relative lower high temperature strength near the Si_3N_4-Mg_2SiO_4 tie line is that if all of the Mg_2SiO_4 is not crystalline, one would expect larger amounts of a relatively fluid silicate to be present in these materials at high temperatures relative to materials with compositions approaching either the Si_3N_4-Si_2N_2O or Si_3N_4-MgO tie lines.

4.3 Oxidation

As recently pointed out by Lange, et al[14] for the case of the Si_3N_4-SiO_2-Y_2O_3 system, the oxidation resistance of hot-pressed Si_3N_4 must be viewed in terms of the compatibility of SiO_2 and Si_2N_2O (the oxidation products of Si_3N_4) with the secondary phases. From an oxidation standpoint, the most desirable secondary phase would be the highest metal-silicate, viz., SiO_2 would not react with the highese silicate until the eutectic temperature between these two phases (SiO_2 and the highest silicate) is reached.

The highest magnesium silicate is $MgSiO_3$. Since the Si_3N_4-$MgSiO_3$ tie line was not observed (see Fig. 1), $MgSiO_3$ is excluded as an equilibrium secondary phase in Si_3N_4 materials hot-pressed with the aid of MgO. The oxidation product of Si_3N_4, e.g., SiO_2, can react in the solid state with the secondary phases, viz., Mg_2SiO_4 and MgO, by

$$Si_3N_4 + 3O_2 \rightarrow 3SiO_2 + 2N_2, \quad (1)$$

$$SiO_2 + 2MgO \rightarrow Mg_2SiO_4, \quad (2)$$

and/or

$$SiO_2 + Mg_2SiO_4 \rightarrow 2MgSiO_3, \quad (3)$$

to eventually form polyphase SiO_2 and $MgSiO_3$ surface scales by solid state diffusional processes. Thus, although other factors must be considered, e.g., reaction kinetics of Eq. (1), (2), and (3), low eutectic temperatures in the Si_3N_4-SiO_2-MgO system, and the ability of the SiO_2 + $MgSiO_3$ scale to act as a diffusional barrier for oxygen, the non-compatibility of SiO_2 with the secondary phase(s) must be considered as an important driving force to decrease the oxidation resistance of Si_3N_4 densified with the aid of MgO.

4.4 Optimization of Strength and Oxidation Resistance

From the data presented in Figs. 2 and 4, it can be seen that optimum strength and oxidation resistance can be obtained with compositions fabricated with high mole fractions of Si_3N_4 ($\geq$ 0.91) and a MgO/SiO_2 molar ratio between 0.25 and 0.50. Material with a better oxidation resistance, but a slightly lower strength, can be fabricated with a MgO/SiO_2 molar ratio of $\sim$0.17. It should be noted that when such small amounts of MgO are used for densification, knowledge of the SiO_2 content in the Si_3N_4 powder and its loss or gain during fabrication are keys to the control of composition and thus, properties.

ACKNOWLEDGMENTS

The author would like to thank R. C. Kuznicki for his help in obtaining the x-ray diffraction patterns and J. J. Nalevanko for his technical assistance.

REFERENCES

1. F. F. Lange, "Task I: Fabrication, Microstructure and Selected Properties of SiALON Compositions," Final Rept. NAVAIR N00019-73-C-0208, Feb. 26, 1974.
2. S. Wild, P. Grieveson and K. H. Jack, Special Ceramics 5, p. 385, Ed. by P. Popper, B.C.R.A. Stock-on-Trent, 1972.
3. I. Kohatsu and J. W. McCauley, Mat. Res. Bull. 9, 917, 1974.
4. K. Kato, et al., J. Am. Ceram. Soc. 58, 90, 1975.
5. H. F. Priest, F. C. Burns, G. L. Priest and E. C. Skaar, J. Am. Ceram. Soc. 56, 395, 1973.
6. A. J. Edwards, D. P. Elias, M. W. Lindley, A. Atkinson, and A. J. Moulson, J. Mat. Sci., 9, 516, 1974.
7. D. Campos-Loriz and F. L. Riley, J. Mat. Sci., 11, 195, 1976.
8. G. G. Deeley, Brit. Pat. No. 942,082, Nov. 20, 1963; G. G. Deeley and N. C. Moore, Powder Met. No. 8, 145, 1961.
9. L. J. Gauckler, H. L. Lukas and G. Petzow, J. Am. Ceram. Soc., 53, 346, 1975.
10. Y. Oyama and O. Kamigaito, Yogyo-Kyokai-Shi, 81, [7], 34, 1973.
11. K. H. Jack, J. Mat. Sci., 11, 1135, 1976.
12. J. L. Iskoe, F. F. Lange, and E. S. Diaz, J. Mat. Sci., 11, 908 1976.
13. L. J. Gauckler, H. L. Lukus, and T. Y. Tien, Mat. Res. Bull., 11, 503, 1976.
14. F. F. Lange, S. C. Singhal and R. C. Kuznicki, "Phase Relations and Stability Studies in the Si_3N_4-SiO_2-Y_2O_3 Pseudo-Ternary System," Tech. Rept. No. 6, ONR N00014-74-C-0284, April 1, 1976.

TABLE 1

Spectrographic Analyses of Westinghouse Si_3N_4 Starting Powder (wt %)

Al	0.08
Ag	< 0.001
B	0.001
Ca	0.016
Cr	0.01
Fe	> 0.1
Mg	0.001
Mn	0.05
Mo	< 0.003
Ni	< 0.01
Pb	< 0.01
Sb	< 0.01
Sn	< 0.01
Ti	0.01
V	0.005
Zn	< 0.01

FIGURE CAPTIONS

Fig. 1 Tie lines observed for hot-pressed compositions in the Si_3N_4-Si_2N_2O-Mg_2SiO_4-MgO portion of the Si_3N_4-SiO_2-MgO system. Closed circles represent materials examined by x-ray diffraction.

Fig. 2 Flexural strength at 25°C and 1400°C vs MgO/SiO_2 molar ratio for compositions containing a) 0.91 mole fraction Si_3N_4, b) 0.833 mole fraction Si_3N_4, and c) 0.755 mole fraction Si_3N_4.

Fig. 3 Oxidation results for representative materials containing 0.755 mole fraction Si_3N_4 and different MgO/SiO_2 molar ratios exposed to air at 1375°C plotted to examine the parabolic rate law, viz., weight gain squared vs time.

Fig. 4 Total weight gain after 785 hrs exposure to air at 1375°C for three series of Si_3N_4 materials vs MgO/SiO_2 molar ratio.

Curve 686272-A

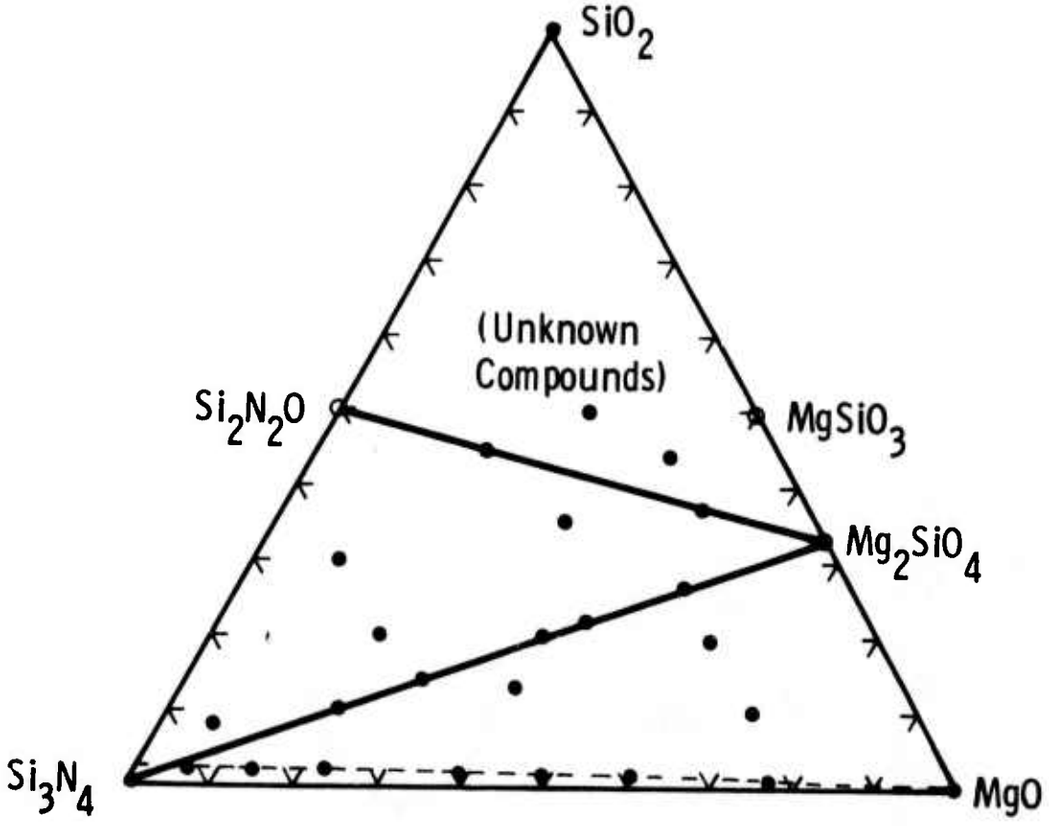

Fig. 1

Curve 686270-A

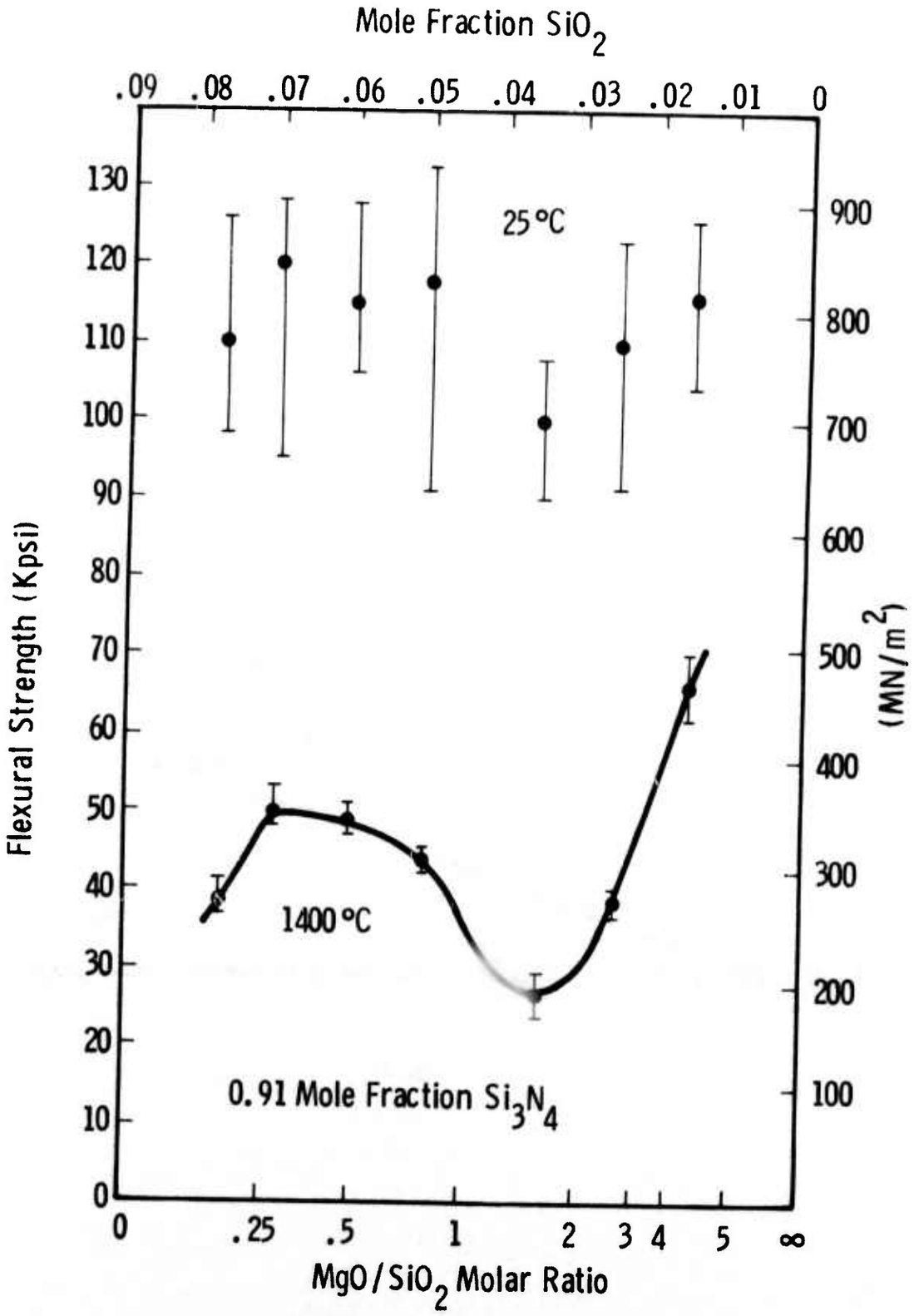

Fig. 2a

Curve 686271-A

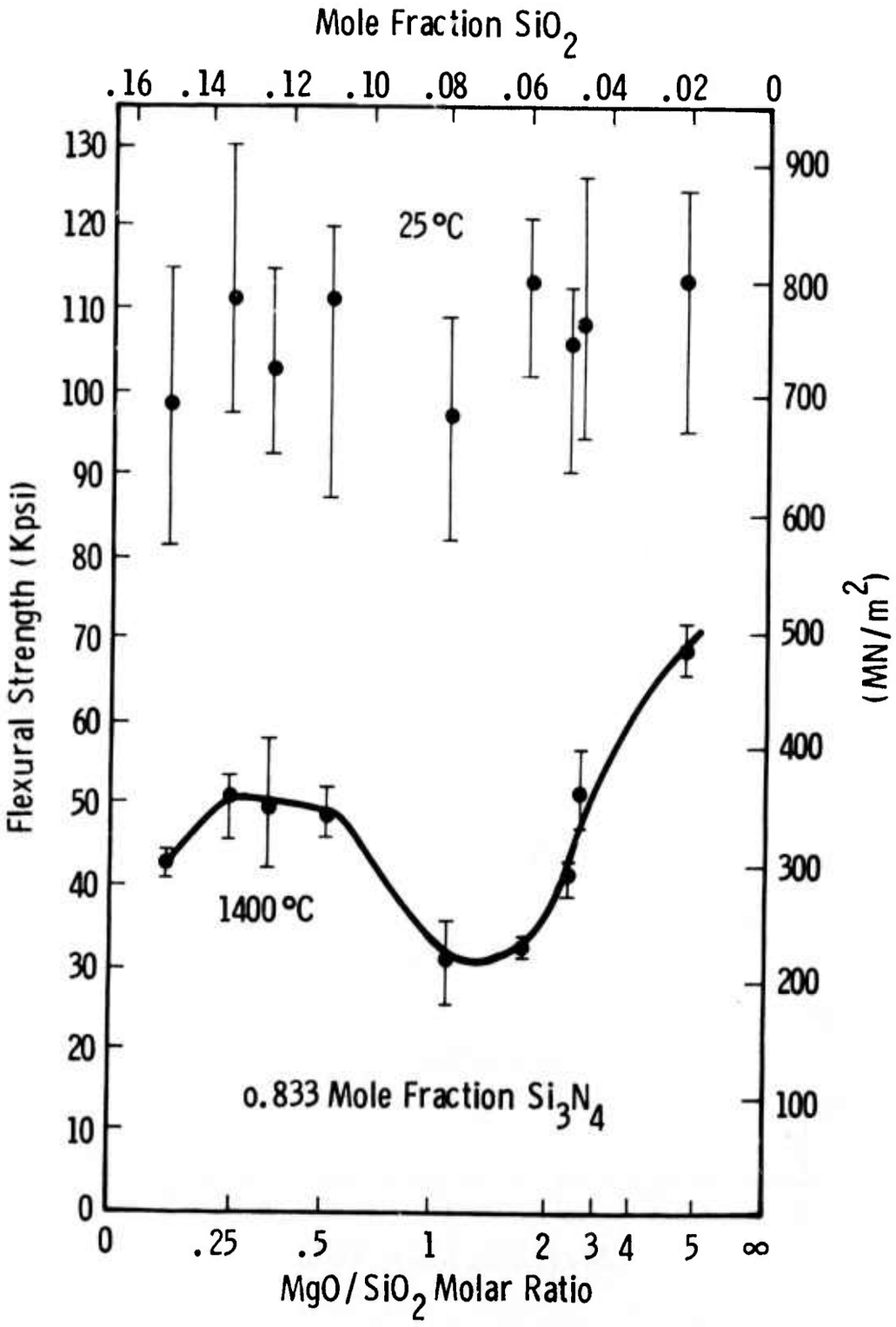

Fig. 2b

Curve 686269-A

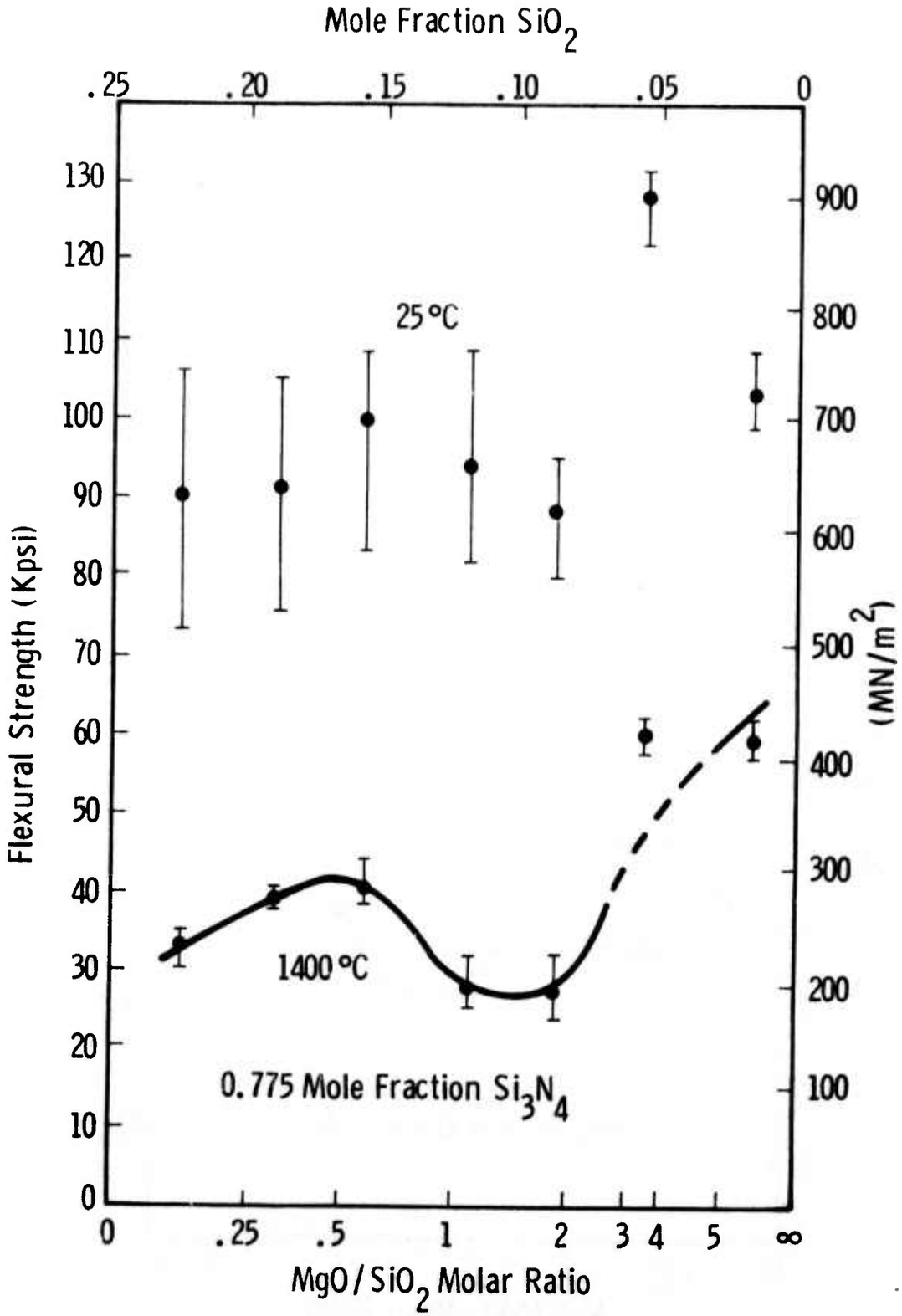

Fig. 2c

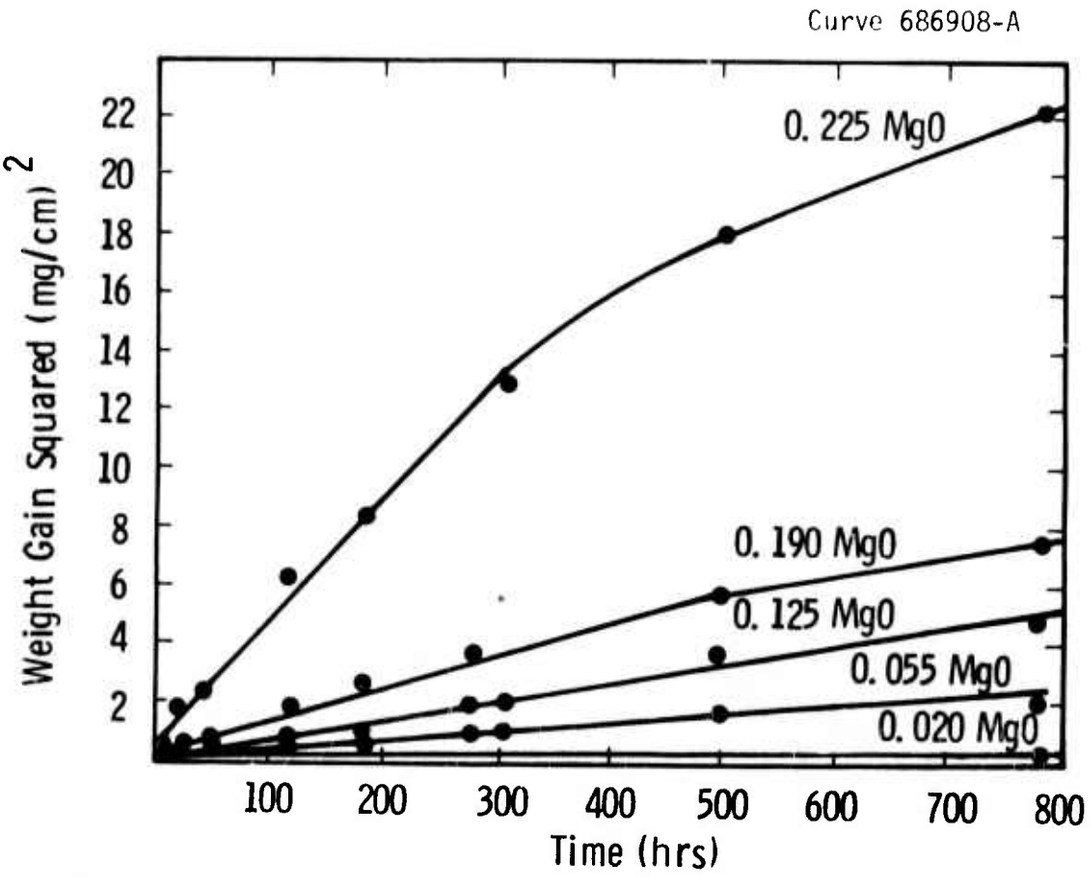
Curve 686908-A
Weight Gain Squared (mg/cm)^2
22
20
18
16
14
12
10
8
6
4
2
0. 225 MgO
0. 190 MgO
0. 125 MgO
0. 055 MgO
0. 020 MgO
100
200
300
400
500
600
700
800
Time (hrs)

Fig. 3

Curve 686907-A

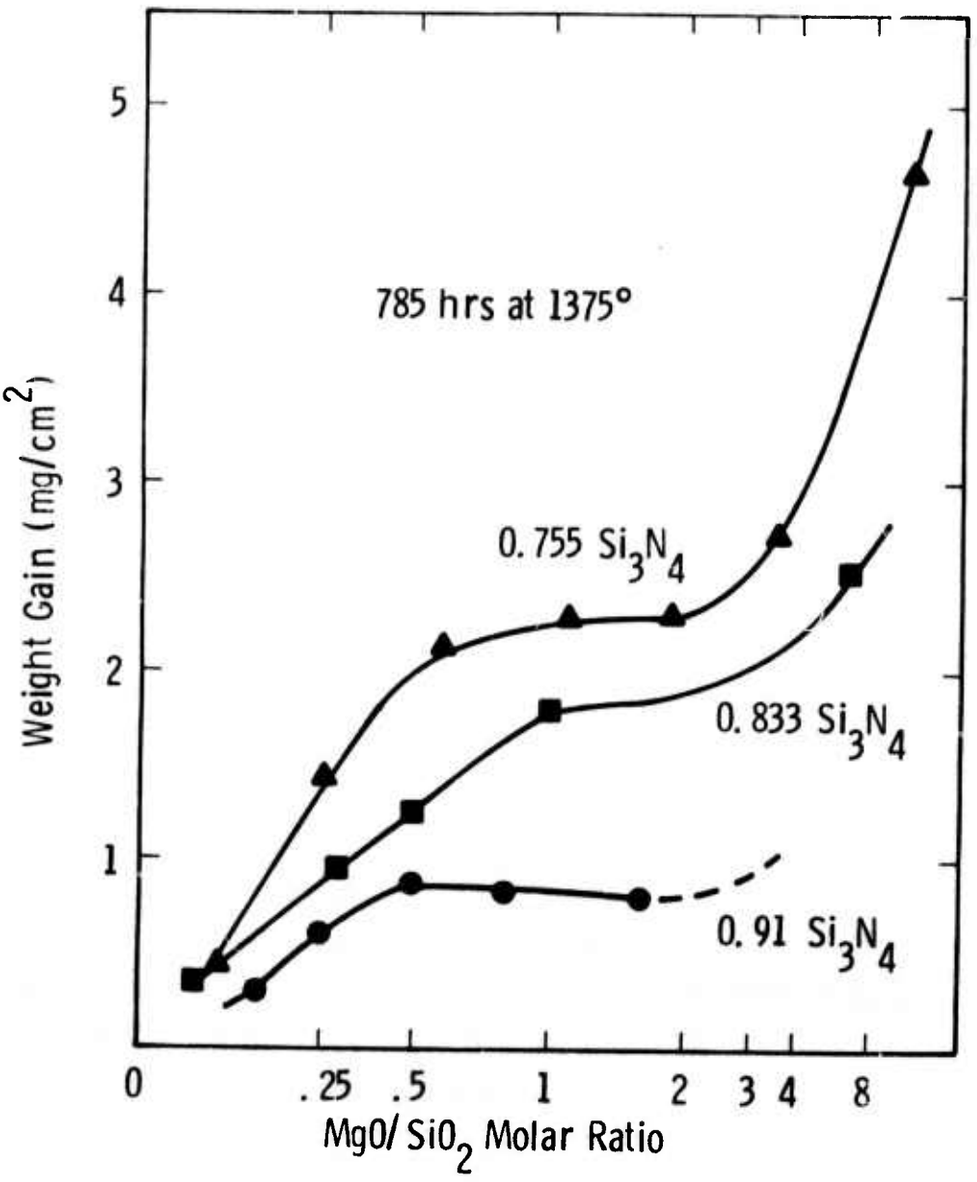

Fig. 4

DENSE Si_3N_4: INTERRELATION BETWEEN PHASE EQUILIBRIA, MICROSTRUCTURE AND MECHANICAL PROPERTIES

F. F. Lange

FINAL REPORT - September 30, 1976

Westinghouse Electric Corporation
Research and Development Center

Contract Number N00014-74-C-0284

Sponsored by the Advanced Projects Agency
ARPA Order Number 2697
Program Code Number 01269

Scientific Officer: Dr. A. M. Diness
Office of Naval Research

Principal Investigator: Dr. F. F. Lange
(412) 256-3554

Effective Date of Contract: April 1, 1974

Contract Expiration Date: June 30, 1976

Amount of Contract: $159,892

Form Approved, Budget -- No. 22-R0293

Unclassified

SECURITY CLASSIFICATION OF THIS PAGE *(When Data Entered)*

REPORT DOCUMENTATION PAGE		READ INSTRUCTIONS BEFORE COMPLETING FORM
1. REPORT NUMBER	2. GOVT ACCESSION NO.	3. RECIPIENT'S CATALOG NUMBER
4. TITLE *(and Subtitle)* Dense Si_3N_4: Interrelation Between Phase Equilibria, Microstructure and Mechanical Properties		5. TYPE OF REPORT & PERIOD COVERED FINAL REPORT September 30, 1976
		6. PERFORMING ORG. REPORT NUMBER
7. AUTHOR(s) F. F. Lange		8. CONTRACT OR GRANT NUMBER(s) N00014-74-C-0284
9. PERFORMING ORGANIZATION NAME AND ADDRESS Westinghouse Research Laboratories Beulah Road Pittsburgh, PA 15235		10. PROGRAM ELEMENT, PROJECT, TASK AREA & WORK UNIT NUMBERS
11. CONTROLLING OFFICE NAME AND ADDRESS Dr. A. M. Diness Office of Naval Research Arlington, VA 22217		12. REPORT DATE September 30, 1976
		13. NUMBER OF PAGES 29
14. MONITORING AGENCY NAME & ADDRESS*(If different from Controlling Office)*		15. SECURITY CLASS. *(of this report)* Unclassified
		15a. DECLASSIFICATION/DOWNGRADING SCHEDULE

16. DISTRIBUTION STATEMENT *(of this Report)*

Reproduction in whole or in part is permitted for any purpose of the U.S. Government. Distribution of this document is UNLIMITED.

17. DISTRIBUTION STATEMENT *(of the abstract entered in Block 20, if different from Report)*

18. SUPPLEMENTARY NOTES

19. KEY WORDS *(Continue on reverse side if necessary and identify by block number)*

Silicon nitride, hot pressing, fabrication, microstructure, strength, creep, phases, equilibrium.

20. ABSTRACT *(Continue on reverse side if necessary and identify by block number)*

The mechanical properties of dense Si_3N_4 will be reviewed from the viewpoint of related fabrication parameters and compositional content. It will be shown that the microstructure of dense Si_3N_4 is governed by the phase relations of the constituents in the starting powder and that these phase relations, in turn, govern the mechanical behavior.

DD FORM 1 JAN 73 1473 EDITION OF 1 NOV 65 IS OBSOLETE

Unclassified

SECURITY CLASSIFICATION OF THIS PAGE *(When Data Entered)*

DENSE Si_3N_4: INTERRELATION BETWEEN PHASE EQUILIBRIA, MICROSTRUCTURE AND MECHANICAL PROPERTIES

F. F. Lange

ABSTRACT

The mechanical properties of dense Si_3N_4 will be reviewed from the viewpoint of related fabrication parameters and compositional content. It will be shown that the microstructure of dense Si_3N_4 is governed by the phase relations of the constituents in the starting powder and that these phase relations, in turn, govern the mechanical behavior.

1. INTRODUCTION

Powder routes are used to fabricate dense Si_3N_4. Deeley[1] was the first to discover that pore-free bodies could be fabricated by hot pressing Si_3N_4 powder containing a densification aid. Many metal oxides, e.g., MgO, BeO, Al_2O_3, Y_2O_3, CeO_2, etc. are known densification aids.[1-4] Although hot pressing currently results in a superior product, the feasibility of pressureless sintering, with incorporated densification aids, has been demonstrated.[5-7]

Densification of Si_3N_4 powder with the aid of a metal oxide is generally attributed to the presence of liquid at high temperatures according to the general reaction:

$$Si_3N_4 + SiO_2 + \text{metal oxide} + (\text{impurities}) \xrightarrow{\text{Temp.}} Si_3N_4 + \text{liquid}, \quad (1.1)$$

where SiO_2 is unavoidably present on the surface of each Si_3N_4 particle and/or incorporated in the powder in the form of Si_2N_2O. Above the solidus temperature, all four constituents of the LHS of (1.1) will react to form a liquid. Neglecting the possible mass losses due to volatilization[5], the composition of the liquid and the equilibrium fraction of solid Si_3N_4 will depend on 1) the composition of the starting powder (i.e., the LHS of Eq. (1.1)), 2) the phase equilibria of the composite system, and 3) the densification temperature. The role of the liquid is to 'pull together' the Si_3N_4 particles and to allow the solution-reprecipitation of Si_3N_4, both of which result in the disappearance of voids and thus, densification.

Upon cooling from the densification temperature, the liquid solidifies according to the general reaction:

$$Si_3N_4 + \text{liquid} \xrightarrow{\text{cooling}} Si_3N_4 + \text{secondary phase}, \quad (1.2)$$

illustrating that Si_3N_4 is a polycrystalline, polyphase material.

The number, chemistry and content of the secondary phases depend on the composition of the starting powder and the phase relations in the given composite system. In addition, the crystal structure of Si_3N_4 can be altered by the concurrent substitution of certain metal cations for silicon and oxygen for nitrogen.[8,9] As experience has shown, the secondary phases and/or the solid solution alloying of Si_3N_4, can significantly influence all properties.

The following text will be split into three interrelated sections: First, fabrication will be reviewed in terms of starting powders, phase relations, the $\alpha \rightarrow \beta$ phase transformation and resulting microstructures. Second, the theoretical effects of second phases on the low and high temperature mechanical properties will be discussed. And, third, the observed relations between microstructure and mechanical properties will be discussed in terms of the starting Si_3N_4 powder, effect of inclusions size, effect of impurities and compositional effects in two Si_3N_4-SiO_2-MgO systems.

2. FABRICATION

2.1 Starting Powders

Silicon nitride exists as two hexagonal crystal structures, viz., α-Si_3N_4 (P31C)[10] and β-Si_3N_4 ($P6_3/m$)[11]. At first, the α and β structures were thought to be, respectively, low and high temperature polymorphs; hence, their designation.[12] Then, based on a structure refinement with x-ray powder pattern data, Jack and co-workers[13] suggested that $\sim$1.5 w/o oxygen was incorporated into the α structure, which led to the conclusion that it was an oxynitride with the approximate formula of $Si_{11.5}N_{15}O_{0.5}$. Previous workers (Marchand, et al[11]) and later workers (Kohatsu and McCauley[14] and Kato, et al[15]) used single crystal x-ray data to refine the α structure. These three groups concluded that the α structure consisted of only Si and N atoms. Numerous workers[7,16,17,18] have also shown that α-Si_3N_4 powder can have much lower oxygen contents than that hypothesized by Jack, e.g., Kato, et al[15] report on oxygen content of 0.05 w/o. Thus, most current workers believe that both α and β structures can be pure Si_3N_4. Although several suggestions have been made,* the thermodynamic interrelation between the two structures is still unknown.

The oxygen content of different Si_3N_4 powders ($\alpha/\beta > 8$) has been reported to range between 0.5 - 3.0 w/o, depending on the manufacturer and the particular batch.[7] Assuming that all the oxygen is present as SiO_2, the SiO_2 molar fraction can range between 0.02 to 0.12, with commercial Si_3N_4 powders in the higher end of this range. Thus, SiO_2 is an important constituent in the starting powder.

---

*Observations indicate that the α structure is formed by a vapor reaction which lead Blegan[19] to suggest that α is metastable at all temperatures.

The major cation impurities in Si_3N_4 powder are Fe, Ca and Al, reflecting the impurities in the raw Si used to manufacture Si_3N_4 and a possible metal addition to promote the nitriding of Si powder.[20] The content of the major impurities can range between 10-5000 ppm (e.g., the range for Ca), depending on the purity of the raw Si prior to nitriding. A microprobe analysis of various Si powders by the author has indicated that the three major impurities can exist as oxides, silicates, and with the exception of Al, as silicides.[21] The effect of impurities on the mechanical properties will be reviewed in section 4.3.2.

The conventional method of preparing Si_3N_4 powder (containing SiO_2 and impurities) for densification consists of mixing in the MO densification aid and reducing the particle size of the composite powders by wet ball milling. Milling can be carried out in containers which will not add additional contaminates except volatile hydrocarbons. The commonly used WC milling media is known to contaminate the powders. Much of the WC contamination can be removed by subsequent classification.[22] Dry alcohols are used during milling to minimize the hydrolization of Si_3N_4 to SiO_2. Measurements before and after milling have shown a negligible change in oxygen content.

Thus, the constituents of the starting 'Si_3N_4' powder are Si_3N_4 ($\alpha/\beta > 8$), metal oxide, and various impurities (Fe, Ca, Al, WC and hydrocarbons).

2.2 Phase Relations

Phase equilibrium studies of various Si_3N_4-oxide systems are only recent and in many cases, SiO_2 was an unrecognized component. As pointed out by Gauckler et al[8] one can not apriori consider any Si_3N_4-SiO_2-MO system an ordinary ternary system,* but if the reciprocal reaction $Si_3N_4 + 6/x\ M_2O_x = 3SiO_2 + 4/x\ M_3/N_x$ (where x = the valence state of the metal ion) can be assumed the system can be represented by a square diagram

*That is, a true binary may not exist along the Si_3N_4-MO join.

with Si_3N_4, $3SiO_2$, $6/x\ M_2O_x$ and $4/x\ M_3N_x$ located at the four appropriate corners. The composition at each point within the diagram can be represented by an equivalent cation concentration (e.g., $[M^{+x}]$), and an equivalent anion concentration (e.g., $[O^{-2}]$). Such phase representation has been reported to illustrate the tie lines observed at 1750°C for the Si_3N_4-Al_2O_3-SiO_2-AlN[8,23] and Si_3N_4-BeO-SiO_2-Be_3N_2[9] systems, and to illustrate the Si_3N_4-MO solid solutions that exist within these systems at a cation/anion ratio of 3/4.

The two important phase diagrams illustrated in Figs. 1 and 2, viz., the Si_3N_4-MgO-SiO_2[24] and Si_3N_4-Y_2O_3-SiO_2[25] systems, are represented in the conventional and more convenient manner. For these two systems, a tie line exists between all or most of the Si_3N_4-MO join. For all practical reasons, this ordinary representation will suffice. The tie lines in both diagrams were obtained by the author (phase identification by x-ray diffraction analysis) for compositions hot pressed at temperatures between 1500-1750°C.* High purity, low oxygen (0.7 w/o) α-Si_3N_4 powder (α/β = 9) was used to obtain these data.

As obviously shown in either diagram, the secondary phases change from one compatibility triangle to another. Not as obvious, but pertinent to material control, the type and amount of each secondary phase can be easily changed for low MO contents when different batches of Si_3N_4 are used which contain different SiO_2 contents. The effect of compositional changes on mechanical properties in these two systems will be described in section 4.3.

2.3 The $\alpha \rightarrow \beta$ Phase Transformation

Investigations have shown that an $\alpha \rightarrow \beta$ phase transformation occurs during fabrication[26-28]. It has also been shown that this transformation occurs both during and after densification, i.e., densification

*Each diagram represents an isothermal section without defined regions of liquid. A constant temperature could not be employed since some compositions would exceed their liquidus temperature and destroy the hot-press dies.

is the more rapid process[27,28]. Simultaneous with the $\alpha \rightarrow \beta$ transformation, the grains transform from an equiaxed to a fibrous, morphology[28], i.e., the microstructure of the fully transformed material with an initial high α content ($\alpha/\beta > 8$), can be described as resembling a log and twig tangle. Observations (e.g., Fig. 3) have suggested that the aspect ratio (R) of the fibrous grains are related to the α/β ratio, i.e., $R = 1 + \alpha/\beta$ and that the diameter of the fibers is similar to the size of the β particles within the initial powder.[28] That is, grain growth during and after densification appear to be restricted to growth parallel to the fiber axis. The strength and fracture toughness of material fabricated with either high α or high β phase powders are discussed in terms of their resulting grain morphologies in section 4.1.

2.4 Resulting Microstructures

As illustrated above, dense Si_3N_4 is a polyphase, polycrystalline material. Evidence for this is not only obtained by x-ray analysis, but also by directly examining the microstructure. Micrographs in Fig. 4 show polished sections of two Si_3N_4 materials fabricated close to the Si_3N_4-MgO tie line (see Fig. 1), illustrating the relative location of the two major phases—in this case, Si_3N_4 and MgO. These microstructures exist below the solidus temperature. (The white phase, viz., the WC contamination, should be neglected for this discussion.)

As illustrated, groups and single grains of Si_3N_4 (lighter phase) are surrounded by MgO (darker phase); this is clearly evident for material containing the larger MgO content (Fig. 4a). As the MgO content decreases (Fig. 4b), the average separation distance between the Si_3N_4 grains (or grain groups) decreases as expected by volume fraction considerations. At lower MgO contents (not shown), the MgO phase is difficult to observe,* but

*Three factors complicate this observation. First, close to the Si_3N_4 corner of the phase diagram, the amount of Mg_2SiO_4 in the material increases due to the fixed amount of SiO_2 in the starting Si_3N_4 powder. Second, as shown on the micrographs, the volume fraction (VF) of MgO in Si_3N_4 is much smaller than the mole fraction (MF), due to the relatively low molecular weight of MgO, viz., VF (MgO) = 11.2 MF(MgO)/[44 MF(Si_3N_4) + 11.2 MF(MgO)]. Third, if all Si_3N_4 grains were equally spaced by the MgO phase, the separation distance $S_o \sim VF/3(1-VF)\ D$; when the grain size (D)$\sim$1 μm, and VF = 0.1; $S_o \gtrsim 400$ Å[29].

observers using electron optics have detected noncrystalline second phases between the grains in such materials.[30-32]

Above the solidus temperature, these same microstructures will, after reaching equilibrium conditions, look different. The MgO will react with Si_3N_4 to form a liquid and residual Si_3N_4, i.e., the amount of second phase between the Si_3N_4 grains (or grain groups) will increase as the temperature increases above the solidus temperature.

Both the effect of solid second phases below the solidus and the presence of liquid second phases above the solidus will be discussed in later sections.

Other microstructural features important for strength considerations are laminar inclusions of second phases resulting from density variations in pre-compacted powders,[33] voids formed by rapid sintering, incomplete sintering, etc., and inclusions accidentally incorporated prior to densification. Only the last feature will be discussed later.

3. THEORETICAL EFFECT OF SECOND PHASES ON MECHANICAL PROPERTIES

3.1 Secondary Phases as Inclusions

One question that arises when observing a microstructure containing secondary phases is: "What is their effect on strength?" This question arises because residual stresses are associated with secondary phases and second-phase inclusions are occasionally located at fracture origins.

The details describing the residual stresses associated with spherical, second-phase inclusions are described elsewhere for the case of differential thermal contraction upon cooling from a fabrication temperature.[34] Other causes for stresses arising around and within second phase inclusions are phase transformation and, when under stress, differential elastic properties. In effect, all inclusions are stress risers and probable locations of cracks, i.e., inclusions are crack precursors.

The effect of second phase inclusions, as found in particulate composites, on strength, fracture toughness and elastic properties has been previously reviewed by the author.[35] The subject enlarged upon here is the dependence of inclusion size on its effectiveness as a crack precursor.

The formation of cracks adjacent (or within) inclusions during the cooling of a given particulate-matrix combination have been observed to depend on the size of the inclusions, viz., cracks are observed to be associated with large inclusions and not with small inclusions.[36,37] This size effect was explained after analyzing the thermodynamics of crack extension and arrest in the highly localized stress field associated with an inclusion.[38]

The analysis for crack extension was based on the fact that the two energy terms that change during cracking, viz., the strain energy within and around the inclusion and the energy associated with the surface formed by the crack, have different functional dependences on the particle size (D). That is, the strain energy term depends on the volume under stress (D^3) and the surface energy term is proportional to the surface of the particle (D^2). By determining the change in these two terms with changing crack length and by invoking Griffith's condition for fracture, the extension of a small pre-existing crack was found to be dependent on both the maximum stress (σ_m) at the inclusion-matrix interface and on the inclusion size (D), i.e., crack extension would only occur when

$$\sigma_m^2 D \geq \text{constant}, \tag{3.1}$$

where the factors included within the constant are material properties and dimensionaless quantities related to the pre-existing crack.[38] Expressed in another manner, the analysis shows that for a given maximum stress (σ_m), a critical particle size exists (D_c) below which cracking will not occur:

$$D_c = \frac{\text{constant}}{\sigma_m^2}. \tag{3.2}$$

Although this analysis is not rigorous for the geometries of the polyphase regions within the Si_3N_4 considered here, it suggests that the size of the second phase regions (and the Si_3N_4 grains themselves) as well as their thermal and elastic properties (which determine the residual stresses) is an important factor in determining the basic strength of these polyphase materials.

Strength measurements of different Si_3N_4-SiC composite materials[39] and SiC-Al_2O_3 composite materials[40] indicate that no strength degradation is observed when the size of the secondary phase regions is approximately the same as the grain size of the matrix. These observations along with the theoretical arguments outlined above suggest that when the second phase

regions are smaller than the Si_3N_4 grains, they will not significantly degrade the basic strength of the material.

3.2 Mechanical Behavior at Elevated Temperatures

Most of measurements and observations have shown that the mechanical properties of hot-pressed Si_3N_4 begin to degrade at elevated temperatures. The contributions of dislocation motion and of solid-state diffusion related phenomena on degradation are uncertain, but overwhelming evidence strongly suggests that the presence of a liquid (or viscous) phase between the Si_3N_4 grains is a major contribution to degradation. The reaction of the secondary phases with Si_3N_4 above the solidus temperature and/or the rapid increase in fluidity of metastable silicate glasses are likely reasons for a liquid between Si_3N_4 grains (or grain clusters).

Two models have been hypothesized to suggest how a liquid may influence the mechanical behavior of a solid-liquid composition. In both models, the liquid is a minority phase and it is located between rigid grains of the solid.

The model proposed by Stocker and Ashby[41] suggests that ". . . the liquid phase enhances creep by providing regions, or paths of high diffusion conductance." Applied shear stresses are visualized to set up chemical potential gradients due to localized high stresses (e.g., at points where grains are in contact), causing the solution and reprecipitation of solid which permits the stored strain energy to dissipate as work. In this case, the liquid phase provides channels of fast material transport. The strain rate function for this model is the same as described for the conventional diffusional flow mechanism except that the effective diffusivity must include the properties and volume content of the liquid. This model suggests no difference for deformation rates in tension and composition.

In the model proposed by Lange[29], diffusion (within the liquid or solid) is neglected, and the mechanics of non-elastic deformation are visualized as due to the separation and sliding of the grains. This model is discussed in the following paragraphs.

Grain boundary sliding is first brought to mind when visualizing a stressed polycrystal with a viscous 'grain boundary phase.' But, if the grains are considered to be relatively rigid, accommodation for grain boundary sliding must be eventually met by the separation of grains. The question then becomes, which is the rate controlling step, the grain boundary sliding or grain boundary separation? Based on theories of liquid adhesives, it was shown that at small strains ($\varepsilon < .1$) and for small volume fractions of the liquid ($VF \leq 0.1$), grain boundary separation was the rate controlling step in the mechanics of deformation, and that the volume fraction of the liquid phase was a dominate microstructural feature. In addition, the growth of vapor bubbles rather than flow of liquid from one part of the material to another was shown to be required for boundary separation. When these important results were combined with fracture mechanics concepts, it was shown that the deformation rate should be significantly greater in tension than in compression.

It was also pointed out that deformation zones would arise in the highly stressed region of a crack front and that such materials will exhibit slow crack growth due to the separation of sliding of grain pairs ahead of pre-existing cracks. Homogeneous deformation within the material, large deformations within the zones associated with cracks and the slow growth of cracks (which leads to a change in compliance) will all contribute to the apparent non-elastic strain.

It is likely that contributions toward non-elastic deformation may be attributed to both models discussed above, but experimental evidence shows that the deformation rate is significantly larger in tension than in compression for both Si_3N_4 [42] and glass ceramics [43] at elevated temperatures. These observations strongly suggest that a mechanism similar to that of separation and sliding appears to be dominate.

4. OBSERVED RELATIONS BETWEEN MICROSTRUCTURE AND MECHANICAL PROPERTIES

4.1 α and β Starting Powders; Strength Anisotropy

All evidence has shown that α starting powder ($\alpha/\beta \geq 8$) consistently leads to high strength hot-pressed Si_3N_4, whereas β starting powder ($\alpha/\beta \leq .1$) only results in moderate strengths. Lange[44] has shown that the critical stress intensity factor (K_c) for materials fabricated with either α or β powders are 6.5 $MN \cdot m^{-3/2}$ and 3.2 $MN \cdot m^{-3/2}$, respectively. As expected from these data, the strength of these materials also differed by a factor of two. Concurrent microstructure observations lead to the hypothesis that the relative high strength and fracture toughness of material fabricated with α powder was due to the fiber-like grain structure of this material relative to the equiaxed grain structured development with the β powder (see Fig. 3). More recent strength and fracture toughness work by Iskoe and Lange[28] for materials where the $\alpha \rightarrow \beta$ phase transformation was incomplete, neither substantiated nor validated the above hypothesis suggesting a need for further work in this area.

Recognition that the fracture toughness and strength of Si_3N_4 appeared to be due to its fibrous grain morphology suggested that the fibers may exhibit preferential orientation during hot pressing which, in turn, suggested that the strength of bulk Si_3N_4 may be anisotropic[44]. Subsequent x-ray diffraction experiments showed that the fiber axes (hexagonal, C-axis of the β grains) were preferentially aligned perpendicular to the hot-pressing direction[44]. Subsequent flexural strength (and K_c measurements*) showed that specimens cut and stressed perpendicular

*K_c from specimen in which the crack phase is parallel and perpendicular to the hot-pressing direction were 7.2 $MN \cdot m^{-3/2}$ and 6.5 $MN \cdot m^{-3/2}$ for material fabricated at Westinghouse. The K_c for Norton material (perpendicular direction) ranges between 4.6 and 5.0 $MN \cdot m^{-3/2}$ (44,45).

to the hot-pressing direction were 20% stronger than specimens cut and stressed parallel to the hot-pressing direction[44]. Thus, the weak and strong directions of hot-pressed Si_3N_4 appear to be due to preferred orientation of the fiber-like Si_3N_4 grains.*

4.2 Large Inclusions

Large inclusions accidentally incorporated during powder processing prior to densification are crack precursors as discussed in the last section. The most commonly observed inclusions in hot-pressed Si_3N_4 were WC (or WSi_2), BN and large aggregates of unreacted Si_3N_4. The source of WC was previously discussed; large mill-ball chips are not uncommon. Large, hard Si_3N_4 aggregates are present in unclassified Si_3N_4 powder. These aggregates can be transferred through most all powder processing procedures and end up as low density inclusions within the hot-pressed material. Boron nitride coatings on graphite dies are used by some manufacturers to prevent a graphite-Si_3N_4 reaction during densification. Occasionally, BN aggregates become dislodged when Si_3N_4 powder is poured into the die to end up as low density BN inclusions within the hot-pressed material.

The large WC and aggregated Si_3N_4 inclusions can be removed by classifying the powder just prior to densification.° Other means can be taken to eliminate BN inclusions. High density inclusions ($\geq$ 125 μm) can be observed within hot-pressed material by x-radiography[45,47]. Low density inclusions require sonic techniques and they are more difficult to detect[45,47].

---

*Other hot-pressed materials that develop an equiaxed grain morphology, e.g., SiC, do not exhibit strength anisotroph[46].

°Classification appears to be the method used to increase the average strength and to decrease the scatter of strength for the Norton hot-pressed Si_3N_4[22].

4.3 High Temperature Behavior and Effects

4.3.1 General Behavior

The strength and creep resistance of hot-pressed Si_3N_4 degrades at high temperatures. The particular temperature where degradation is first observed depends on compositional effects described below and for the case of strength, the rate in which the specimen is stressed.

The strength dependence on stressing rate at elevated temperature was the first indication that slow crack growth was the cause of strength degradation[48]. One of many different chemical or microstructural mechanisms can be responsible for the growth of pre-existing cracks at velocities and stress intensities much lower than that required to cause catastrophic fracture. Although atmospheric effects have been reported[49], the apparent solid-liquid microstructure of Si_3N_4 appears to be the cause of slow crack growth at elevated temperatures[48,50,51].

Slow crack growth causes time dependent failure, the details of which can be found elsewhere[52,53]. Slow crack growth, and thus time dependent failure, can be characterized by crack velocity (V) vs stress intensity factor (K) measurements. Phenomenological V vs K curves for many ceramic materials have satisfied a simple $V = V_o (K/K_o)^n$ relation[53]. Unfortunately, this relation may not be valid for commercial Si_3N_4 (in effect, n appears to decrease with decreasing velocity), preventing long-term failure prediction, but not influencing material comparisons when the data are obtained over the same velocity range[53].

4.3.2 Effect of Impurities

Impurities were the first compositional factors known to influence the high temperature mechanical properties of hot-pressed Si_3N_4[48,54]. The effect of the major impurities on the strength and creep resistance of hot-pressed Si_3N_4 (approximate molar composition: Si_3N_4 = 0.79; MgO = 0.15; SiO_2 = 0.06) at 1400°C is shown in Fig. 5[55]. To obtain these data, the impurities were added as oxides (or carbonates) to relatively pure α-Si_3N_4 powder prior to hot pressing. For the case

where MgO is the densification aid (i.e., material in the Si_3N_4-SiO_2-MgO system), CaO was the most detrimental impurity.* In other systems, other impurities may be important culprits.

4.3.3 Compositional Effects: Si_3N_4-SiO_2-MgO System

The effect of composition was first reported by Andersson, Lange and Iskoe[56] and more thoroughly studied by Lange[24]. As shown in Fig. 6 for compositions containing 0.833 mole fraction Si_3N_4, the strength at 1400°C (and the ratio of strengths at 25°C and 1400°C) are strongly related to the MgO/SiO_2 molar ratio. Exact behavior was also obtained for materials containing both 0.91 and 0.755 mole fractions of Si_3N_4.° The lowest strengths (at 1400°C) were observed for a MgO/SiO_2 molar ratio of 2:1, viz., along the Si_3N_4-Mg_2SiO_4 tie line.† Maximum strength is obtained when $MgO/SiO_2 \rightarrow \infty$, viz., along the Si_3N_4-MgO tie line. High strengths are also observed close to the Si_3N_4-Si_2N_2O tie line. Strengths at 25°C are relatively independent of composition.

It is obvious that the high temperature strength is strongly compositional dependent. Strength appears related to phase equilibria parameters, e.g., the solidus temperature+ but further phase equilibria work (viz., the determination of solidus temperatures) is required for better judgment.

---

*Na_2O and K_2O volatized during fabrication; ∿2/3 of Li_2O disappeared during fabrication[55].

°Lower room temperature strengths (∿15%) were obtained for the 0.755 mole fraction material.

†The non-elastic portion of the stress-strain curve is also a maximum along the Si_3N_4-Mg_2SiO_4 tie line[24].

+Fabrication work in this system suggests a solidus temperature of 1300°C within the Si_3N_4-Si_2N_2O-MgO system[24].

4.3.4 Compositional Effects: Si_3N_4-SiO_2-Y_2O_3 System

Materials in the Si_3N_4-$SiO_2Y_2O_3$ system (see Fig. 2) which contain one or more of the following secondary phases: $Si_3Y_2O_3N_4$, $YSiO_2N$, $Y_{10}Si_7O_{23}N_4$ and/or $Y_4Si_2O_2O_7N_2$ exhibit unusual oxidation behavior and catastrophic strength degradation at elevated temperatures[25].

Detailed oxidation experiments have shown that $Si_3Y_2O_3N_4$ exhibits linear oxidation kinetics, i.e., the oxide surface scale does not protect the $Si_3Y_2O_3N_4$[25]. Preliminary experiments indicate that $YSiO_2N$, $Y_{10}Si_7O_{23}N_4$ and $Y_4Si_2O_7N_2$ also exhibit linear oxidation kinetics[25]. All evidence shows that when these Y-Si-O-N compounds are present as secondary phases, and they preferentially oxidize to cause cracks to develop in the polyphase Si_3N_4 material. Thus, the presence of these four compounds is unwanted.

The four unwanted compounds can be precluded as secondary phases when material in this system is fabricated within the Si_3N_4-Si_2N_2O-$Y_2Si_2O_7$ compatibility triangle[25]. Due to the compatibility of SiO_2 with $Y_2Si_2O_7$ (the highest yittrium silicate), materials within this compatibility triangle also exhibit the best oxidation resistance observed for hot-pressed Si_3N_4 materials.

5. CONCLUDING REMARKS

As illustrated above, both the constituents within the starting powder and the phase relations between these constituents govern the mechanical properties of dense Si_3N_4. Similar to mechanical properties, all other properties are governed by these same relations.

As first shown for the Si_3N_4-SiO_2-Y_2O_3 system, the oxidation behavior of dense Si_3N_4 depends on its composition[25]. Compositions that lie within the Si_3N_4-$Y_2Si_2O_7$-Y_2O_3 area will contain one or more of the unstable compounds, whereas compositions within the Si_3N_4-$Y_2Si_2O_7$-Si_2N_2O compatibility triangle will exhibit unusually good oxidation resistance apparently due to the compatibility of SiO_2 (the oxidation product of Si_3N_4) with $Y_2Si_2O_7$. Namely, from an oxidation viewpoint, the highest metal-silicate is a desirable second phase. Materials densified with the aid of MgO do not have this excellent resistance to oxidation apparently due to the preclusion of the highest silicate (Mg_2SiO_4) by the phase relations (see Fig. 1)[24].

Thermal properties are also governed by the types and amounts of the secondary phases[7]. It has been pointed out that the solid-solution of Al and O in the Si_3N_4 structure is the apparent cause for the lower thermal conductivity of SiAlON materials[57].

Conditions of phase equilibrium have been emphasized in the text. It should be remembered that nonequilibrium conditions may prevail due to the sluggish crystallization kinetics of silicates. Evidence for glassy secondary phases[31-32] and discussions concerning the effect of glassy 'grain boundary' phases on high temperature mechanical properties is found in the literature[29,50,51,54,55]. Although this author does not dispute this viewpoint, it should also be remembered that a liquid will be present in these polyphase materials whenever the solidus

temperature is exceeded. Thus, the determination of solidus and liquidus temperatures for pertinent compositional areas is essential.

In conclusion, it can be seen that the effect of different densification aids and impurities on fabrication, microstructure and properties should be approached through related phase equilibrium studies. Three guide lines can be suggested to achieve improved high temperature structural materials based on Si_3N_4. First, the solidus temperature should be as high as possible to prevent the formation of a liquid within the desired temperature range of application. Second, from an oxidation viewpoint, the secondary phase should be compatible with SiO_2. Third, to minimize thermal stresses (during, e.g., thermal transients), the thermal properties of the secondary phases should not significantly detract from those intrinsic to Si_3N_4. In practice, compromises will be necessary to achieve fabricability.

ACKNOWLEDGMENTS

Thanks are due Westinghouse colleagues who were essential participants in the work reviewed above. Special acknowledgment is due Dr. A. M. Diness, Scientific Officer, Office of Naval Research, for personal support of the effort which led to this review.

REFERENCES

1. G. G. Deeley, Brit. Pat. No. 942,082, Nov. 20, 1963. G. G. Deeley, J. M. Herbert, and N. C. Moore, Powder Met. No. 8, 145, 1961.
2. G. E. Gazza, J. Am. Ceram. Soc., 56, 662, 1973.
3. I. C. Huseby and G. Petzow, Powder Met. Int., 6, 17, 1974.
4. K. S. Kazdiyasni and C. M. Cooke, J. Am. Ceram. Soc., 57, 536, 1974.
5. G. R. Terwilliger and F. F. Lange, J. Mat. Sci., 10, 1169, 1975.
6. K. H. Jack and W. I. Wilson, Nature Phys. Sci. (London) 238, 28, July 10, 1972.
7. F. F. Lange, "Task I: Fabrication, Microstructure and Selected Properties of SiAlON Compositions," Final Report NAVAIR N00019-73-C-0208, Feb. 26, 1974.
8. L. J. Gauckler, H. L. Lukas and G. Petzow, J. Am. Ceram. Soc., 53, 346, 1975.
9. I. C. Huseby, H. L. Lukas and G. Petzow, J. Am. Ceram. Soc., 58, 377, 1975.
10. R. Marchand, Y. Laurent, J. Lang and M. Th. LeBihan, Acta Crys. B25, 2157, 1969.
11. D. Hardie and K. H. Jack, Nature (London) 180, 332, 1957.
12. E. T. Kurkdogan, P. M. Bills and V. A. Tippett, J. Appl. Chem., 8, 296, 1958.
13. S. Wild, P. Grieveson and K. H. Jack, Special Ceramics, 5, pp. 385, Ed. by P. Popper, B.C.R.A., Stoke-on-Trent, 1972.
14. I. Kohatsu and J. W. McCauley, Mat. Res. Bull., 9, 917, 1974.
15. K. Kato, Z. Inque, K. Kijima, I. Kawada, H. Tanaka, and T. Yamane, J. Am. Ceram. Soc., 58, 90, 1975.
16. H. F. Priest, F. C. Burns, G. L. Priest, and E. C. Skaar, J. Am. Ceram. Soc., 56, 395, 1973.
17. A. J. Edwards, D. P. Elias, M. W. Lindley, A. Atkinson, and A. J. Moulson, J. Mat. Sci., 9, 516, 1974.

18. D. Campos-Loriz and F. L. Riley, J. Mat. Sci., 11, 195, 1976.
19. K. Blegen, Special Ceramics, 6, p. 223 (see Ref. 13).
20. T. Yamauchi and H. Suzuki, U. S. Patent 3,206,318, Sept. 14, 1965.
21. F. F. Lange, unpublished work.
22. H. R. Baumgartner and D. W. Richerson, Fracture Mechanics of Ceramics, 1, p. 367, Ed. by R. C. Bradt, D.P.H. Hasselman and F. F. Lange, Plenum, 1974.
23. K. H. Jack, J. Mat. Sci., 11, 1135, 1976.
24. F. F. Lange, "Phase Relations in the Si_3N_4-SiO_2-MgO System: Compositional Effects on Strength and Oxidation Resistance," ONR Tech. Rept. No. 9, Contract N00014-74-C-0284.
25. F. F. Lange, S. C. Singhal, and R. C. Kuznicki, "Phase Relations and Stability Studies in the Si_3N_4-SiO_2-Y_2O_3 Pseudo-Ternary System," Tech. Rept. No. 6, ONR N00014-74-C-0284, April 1, 1976.
26. S. Wild, P. Grieveson, K. H. Jack and M. J. Latimer, Special Ceramics, 5, p. 377, (see Ref. 13).
27. R. J. Weston and T. G. Garruthers, Proc. Brit. Ceram. Soc., No. 22, 197, 1973.
28. J. L. Iskoe and F. F. Lange, "Development of Microstructure, Strength and Fracture Toughness of Hot-Pressed Si_3N_4," Tech. Rept. No. 7, (see Ref. 25).
29. F. F. Lange, Deformation of Ceramic Materials, p. 361, Ed. by R. C. Bradt and R. E. Tressler, Plenum, 1975.
30. J. V. Sharp and A. G. Evans, J. Mat. Sci., 6, 1292, 1971
31. R. Kossowsky, J. Mat. Sci., 8, 1603, 1973.
32. P. Drew and M. H. Lewis, J. Mat. Sci., 9, 261, 1974.
33. F. F. Lange, J. Mat. Sci., 10, 314, 1975
34. J. Selsing, J. Am. Ceram. Soc., 44, 419, 1961.
35. F. F. Lange, "Fracture of Brittle Matrix, Particulate Composites," Composite Materials, 5, pp. 1-44, Ed. by J. L. Broutman, Academic, 1974.
36. D. B. Binns, Science of Ceramics, 1, p. 315, Ed. by G.H. Stewart, Academic, 1972.
37. R. W. Davidge and T. J. Green, J. Mat. Sci., 3, 629, 1968.

38. F. F. Lange, Fracture Mechanics of Ceramics, 2, p. 599, (see Ref. 22).
39. F. F. Lange, J. Am. Ceram. Soc., 56, 445 (1973).
40. F. F. Lange, "Strong, High-Temperature Ceramics," Ann. Rev. Mat. Sci., 4, p. 364, 1974.
41. R. L. Stocker and M. F. Ashby, Rev. Geophysic and Space Phys., 11, 391, 1973.
42. A. F. McLean, E. A. Fisher and R. J. Bratton, "Brittle Materials Design, High Temperature Gas Turbine," AMMRC CTR 73-9, Interim Rept., p. 149, March 1973.
43. R. Morrell and K.H.G. Ashbee, J. Mat. Sci., 8, 1253, 1973.
44. F. F. Lange, J. Am. Ceram. Soc., 56, 518, 1973.
45. R. J. Bratton, C. A. Andersson, F. F. Lange and S. C. Sanday, "Ceramic Rotor Blade Development - 2nd Semi-Annual Tech. Rept.," EPRI Contract No. RP 421-1, May 15, 1976.
46. A. F. McLean, E. A. Fisher and R. J. Bratton, "Brittle Materials Design, High Temperature Gas Turbine," AMMRC CTR 73-32, Interim Rept., p. 154, September 1973.
47. R. Kossowsky, Ceramics for High Performance Applications, p. 665, Ed. by J. J. Burke, A. E. Gorum and R. N. Katz, Brook Hill, 1974.
48. F. F. Lange, J. Am. Ceram. Soc., 57, 84, 1974.
49. D. J. Rowcliffe and P. A. Huber, Proc. Brit. Ceram. Soc., No. 25, 239, 1975.
50. F. F. Lange and J. L. Iskoe, p. 223, (see Ref. 48).
51. A. G. Evans, p. 373 (see Ref. 48).
52. S. M. Wiederhorn, Fracture Mechanics of Ceramics, 2, p. 613, (see Ref. 22).
53. A. G. Evans and S. M. Wiederhorn, J. Mat. Sci., 9, 270, 1974; A. G. Evans, L. R. Russell and D. W. Richerson, Met. Trans. 6A, 707, 1975.
54. D. W. Richerson, Bul. Am. Ceram. Soc., 52, 560, 1973.
55. J. L. Iskoe, F. F. Lange and E. S. Diaz, J. Mat. Sci., 11, 908, 1976.
56. C. A. Andersson, F. F. Lange and J. L. Iskoe, "Effect of MgO/SiO_2 Molar Ratio on High Temperature Strength of Hot-Pressed Si_3N_4," ONR Tech. Rept. No. 3, Contract No. N00014-74-C-0284, Oct 15, 1975.

FIGURE CAPTIONS

Fig. 1 Tie lines observed in the Si_3N_4-SiO_2-MgO system between 1000°C and 1750°C.

Fig. 2 Tie lines observed in the Si_3N_4-SiO_2-Y_2O_3 system between 1500°C and 1750°C.

Fig. 3 Micrographs of etched fracture surfaces of (a) material fabricated with β ($\alpha/\beta \sim 0.1$) Si_3N_4 powder and (b) material fabricated with α ($\alpha/\beta = 9$) Si_3N_4 powder.

Fig. 4 Unetched micrographs of material close to the Si_3N_4-MgO tie line: a) 70 mole % MgO, b) 40 mole % MgO.

Fig. 5 Flexural strength for Si_3N_4 with incorporated oxide impurities.

Fig. 6 Flexural strength of Si_3N_4 (0.833 mole fraction) as a function of the MgO/SiO_2 molar ratio.

Dwg. 6385A70

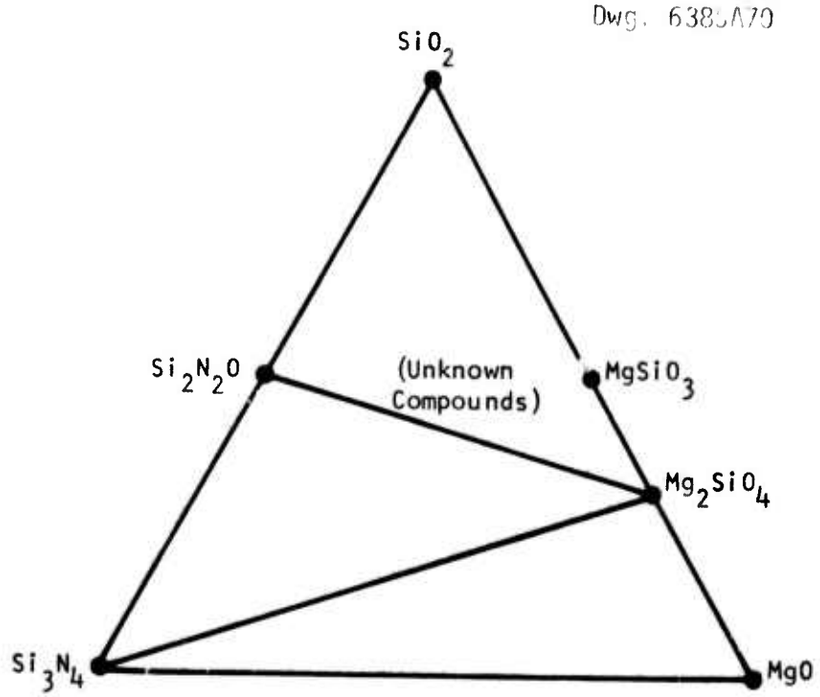

Fig. 1

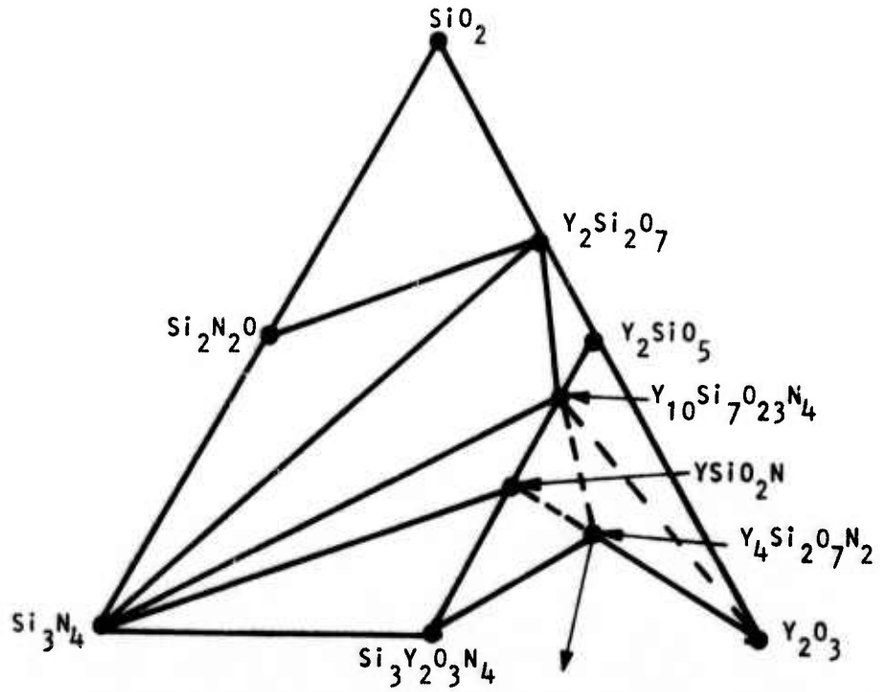

Fig. 2

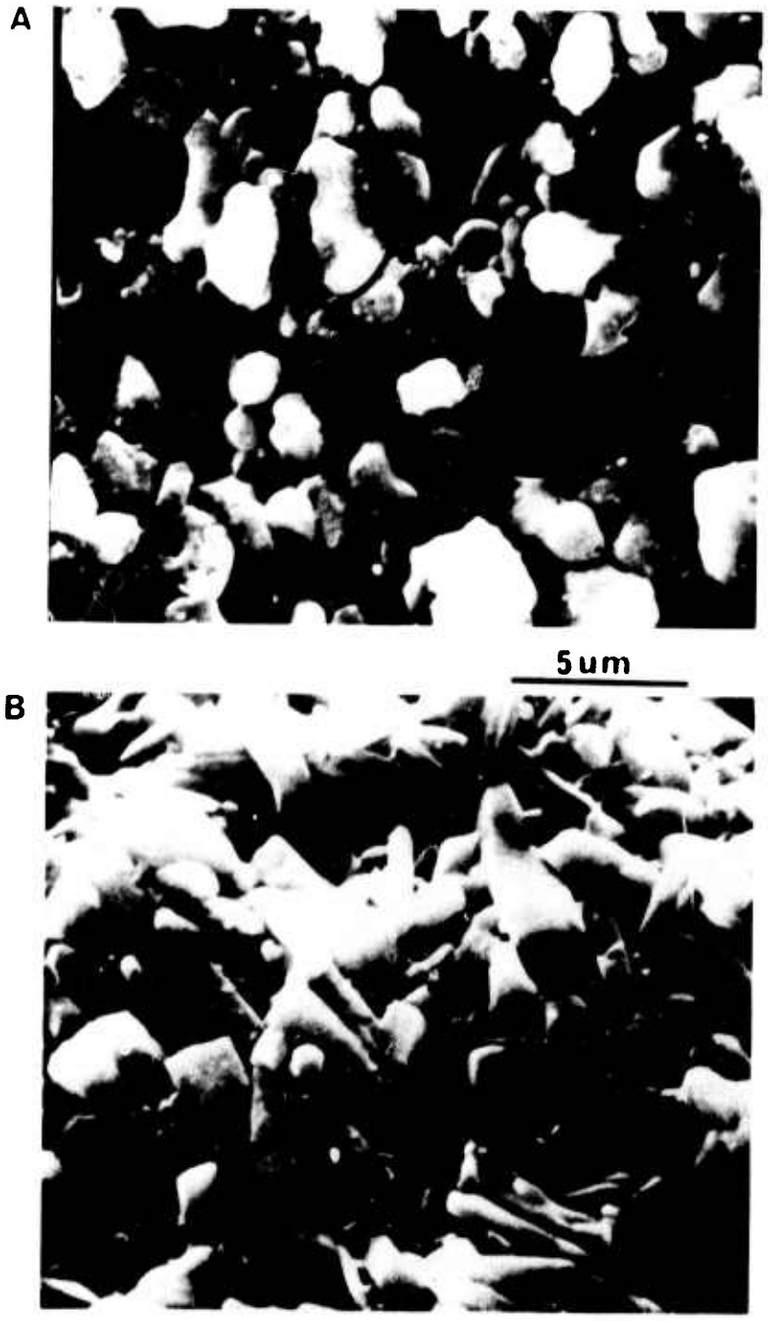

Fig. 3 Micrographs of etched fracture surfaces of (a) material fabricated with β ($\alpha/\beta \sim 0.1$) Si_3N_4 powder, and (b) material fabricated with α ($\alpha/\beta = 9$) Si_3N_4 powder.

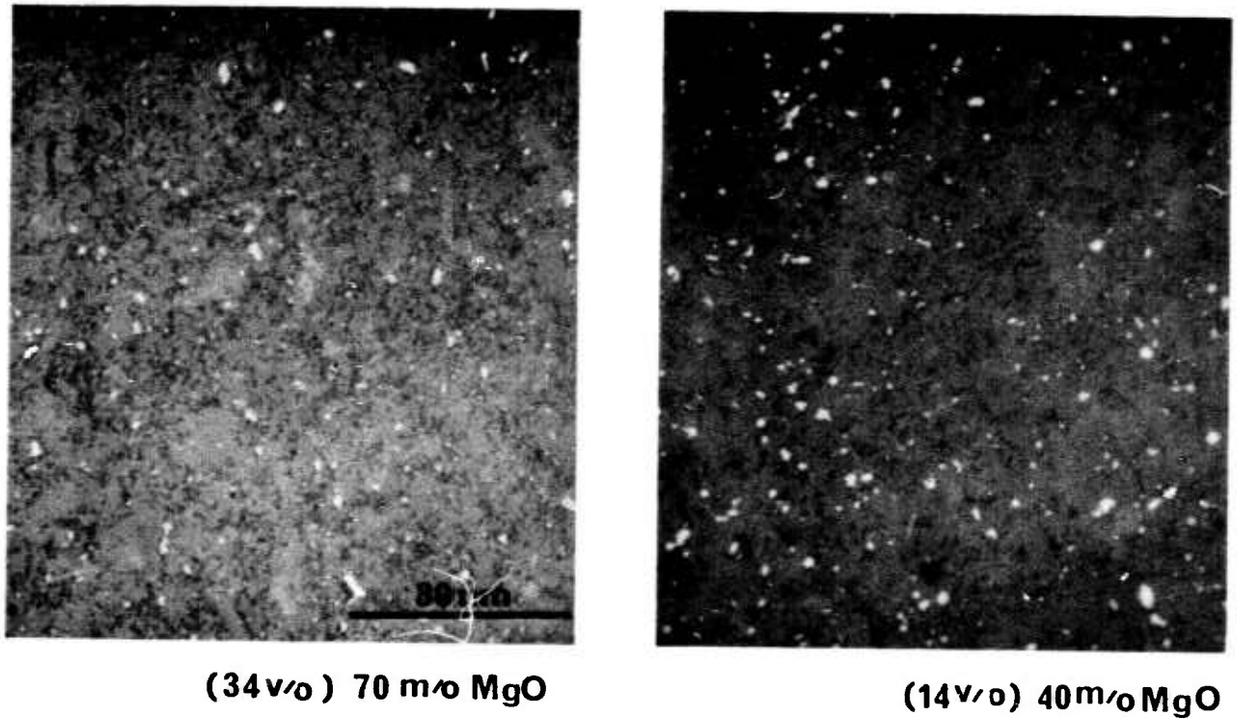

Fig. 4 Unetched micrographs of material close to the Si_3N_4-MgO tie line: a) 70 mole % MgO, b) 40 mole % MgO.

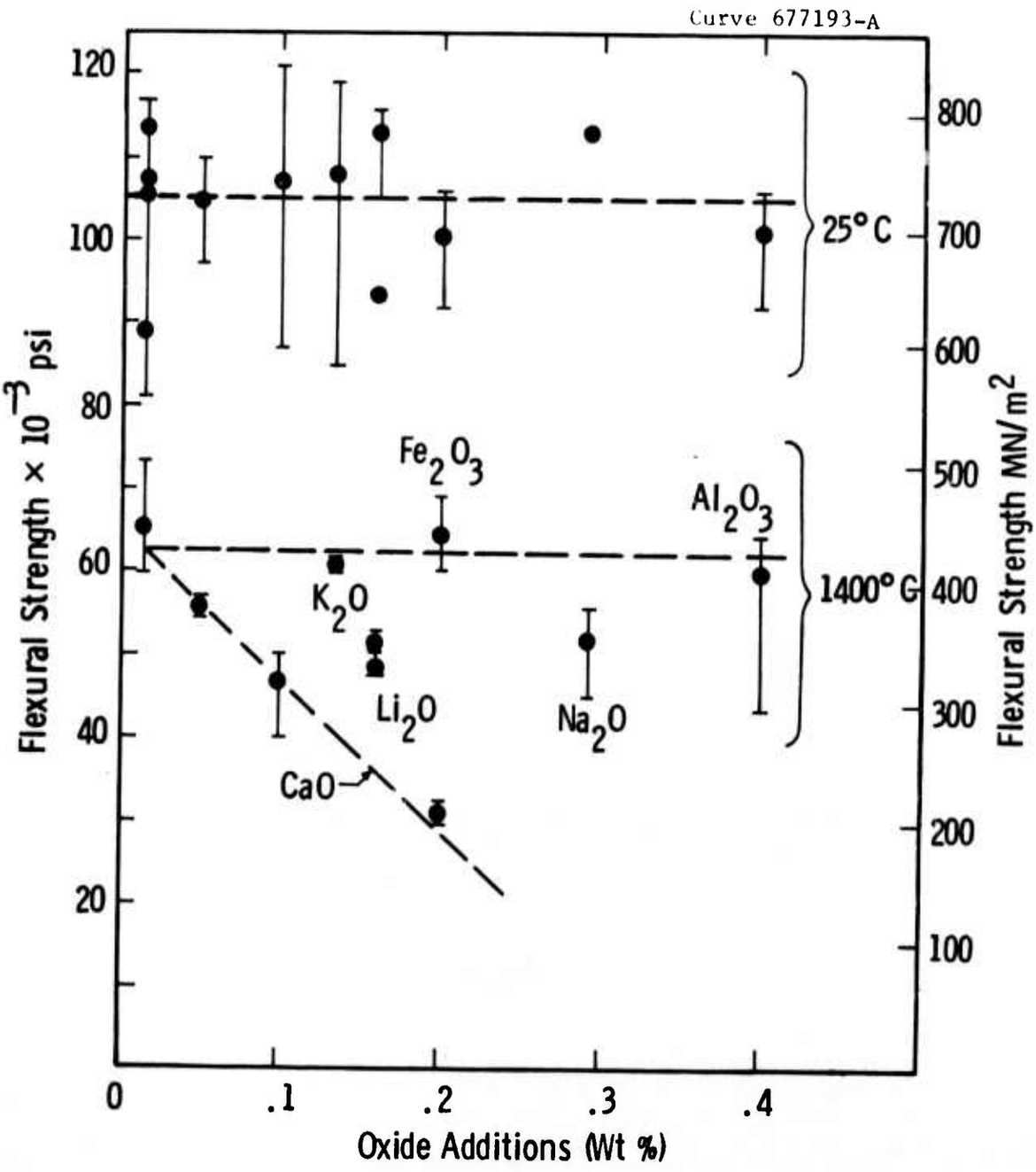
Curve 677193-A
120
100
80
60
40
20
800
700
600
500
400
300
200
100
25° C
1400° G
Fe_2O_3
Al_2O_3
K_2O
Li_2O
Na_2O
CaO
Flexural Strength × 10^{-3} psi
Flexural Strength MN/m^2
0
.1
.2
.3
.4
Oxide Additions (Wt %)

Fig. 5

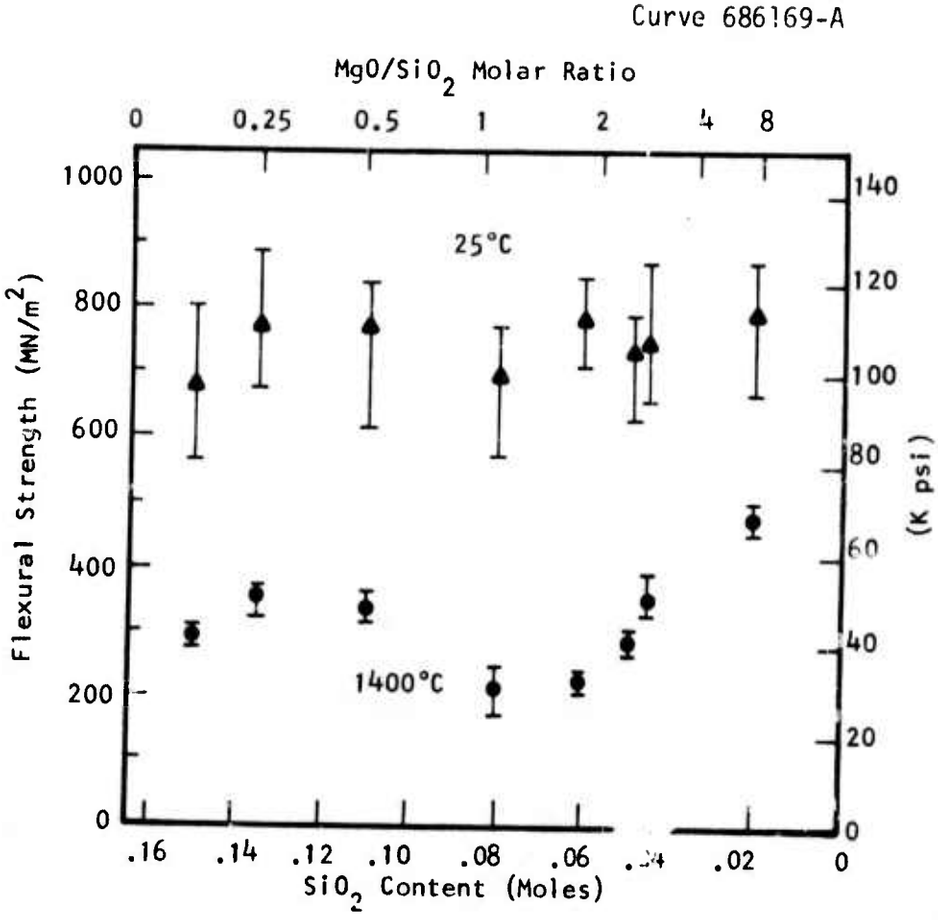
Curve 686169-A
MgO/SiO2 Molar Ratio
0
0.25
0.5
1
2
4
8
1000
800
600
400
200
0
25°C
1400°C
Flexural Strength (MN/m2)
140
120
100
80
60
40
20
0
(K psi)
.16
.14
.12
.10
.08
.06
.04
.02
0
SiO2 Content (Moles)

Fig. 6